Tortuosity and Cementation Exponent as Variables related to Heterogeneity and the Impact on S_w Calculations in Tambaredjo Field of Suriname

Aima Mijland[1], *Elias R.* Acosta[2], and *Mitchel* Pinas[3]

[1]Staatsolie Maatschappij Suriname N.V., Functional Subsurface Support Division / Petrophysics Department, Paramaribo, Suriname
[2]Dunia Technology Solutions assigned to Staatsolie Maatschappij Suriname N.V., Functional Subsurface Support Division / Petrophysics Department, Paramaribo, Suriname
[3]Independent Consultant (former FSS / Petrophysics Department trainee), Paramaribo, Suriname

Abstract. The objective of this research was to propose an alternative method regarding the determination of tortuosity (a) and cementation exponent (m) by finding the best correlation between these parameters and a heterogeneity index using the available core data. Estimate log curves of these parameters and analyze the impact on S_w calculations in the Tambaredjo field.

Core data was used to obtain a relationship between grain and pore size distribution. For grain size distribution, Folk, Moment and Trask indices for sorting were used and plotted against several heterogeneity indices (HI), reservoir properties and pore throat size (PTS) representing pore size distribution. After filtering low regression correlations and non-logical trends, clay volume (V_{cl}), shale volume (V_{sh}), and Basic Petrophysical Property Index (BPPI) were defined as best matches. Equations for each were applied to log data and were evaluated. The ones based on BPPI were selected based on the criteria of depth variations and inverse proportionality between a and m.

Water saturation (S_w) calculations using Indonesian (Poupon & Leveaux) was updated incorporating a and m as variables (log curves), comparing it with S_w from core data and previous calculations using fixed average values (a=1 & m=1.66) from core data. Results show that using a and m as variable parameters improves previous calculations of S_w from 42 to 37% average and delivers a better fit compared to core data.

Even though many studies have been conducted related to a and m determination and their impact on water saturation calculations, still it is a common practice to use average values over a whole field, regardless of heterogeneity considerations. This study proposes a method to include formation heterogeneity in a and m determination, allowing for a more reliable water saturation determination as demonstrated in the Tambaredjo field of Suriname.

1 Introduction

Analysis of petrophysical data of a reservoir is determining the information that facilitate on defining the Stock Tank Oil Initially in Place (STOIIP). Water saturation (S_w) calculated from open-hole resistivity measurements is a primary input for STOIIP estimation. S_w determination is a critical and complex petrophysical calculation, as each S_w equations consist of several parameters, with each having their own uncertainty in their determination.

A correct estimation of Archie's parameters (tortuosity (a) and cementation factor (m)) within a specific reservoir is important as there are considerable variations in texture and pore type, hence these parameters become more sensitive to pore pattern distribution and lithofacies properties [1].

Schon [2] described that the parameters m and a, can be related to the pore geometry (texture) of the rock. Hamada, et al. [1], Attia [3] and Tiab and Donaldson [4] examined the effect of petrophysical rock properties on the lithology factor a and used the tortuosity factor to improve water saturation calculations and regression fitting [5].

During a Reservoir Characterization Study (RCS) of the TAM Central study area [6] S_w calculations were estimated using the Indonesian [7] equation (Equation 1).

$$S_w = \sqrt[n]{\left[\left(\frac{V_{cl}^{2-V_{cl}}}{R_{cl}}\right)^{1/2} + \left(\frac{\emptyset_e^m}{a \times R_w}\right)^{1/2}\right]^2 \times R_t} \tag{1}$$

Where: S_w = water saturation (v/v); V_{cl} = clay volume (v/v); R_{cl} = clay resistivity (ohm.m); $\emptyset_e$ = effective porosity (v/v); R_w = formation water resistivity (ohm.m); R_t = true formation resistivity (ohm.m); m = cementation factor (dimensionless); a = tortuosity factor (dimensionless) and n = saturation exponent (dimensionless).

* Corresponding author: eacosta@staatsolie.com

The calculated S_w values appear not to agree with initial production performances, hence resulting in very low estimated STOIIP and perhaps very high oil recovery. This did not match observed reserves nor expected primary oil recovery.

Correct estimation of the Archie [8] parameters (*a* and *m*) has always been challenging. They are functions of the changes in pore geometry, tortuosity of the pores, formation pressure and clay content. They are inputs of the Indonesian equation (Equation 1) and both are affected by formation lithology. The variable input values of these parameters do impact S_w calculation in a considerable amount if translated to STOIIP estimates as concluded by Lang in 1972 [9]. Therefore, accurate determination of these parameters is required, which is the aim of this study.

In standard formation evaluation, Archie's parameters are usually held constant. Knowing this, the change in lithology per location is not considered when these parameter values are used as constants in a heterogeneous reservoir.

Heterogeneous formations vary in sizes, shapes and distribution of grains and pores. Selecting the correct heterogeneity index related to *a* and *m* values from core data should lead to better representation of changes in formation lithology. Choosing an appropriate index is critical and should be done with caution.

The values of *a* and *m* will be different depending on the approach (free regression fitting or forced regression fitting). As perceived, reservoir samples differ in rock quality, which indicates variation differences in rock quality per well. The heterogeneity distributed over the Tambaredjo field results in different pairs of *a* and *m* for each well. These parameters vary widely and change continuously for each sample due to the changes in lithology depending on the depth [10].

2 Tambaredjo Field (study area)

The study area is the Tambaredjo Central Area (TCA), that is part of the Tambaredjo producing field. This field is in the marshy coastal area of Suriname in the district of Saramacca, about 45 km west of the capital city Paramaribo (Fig. 1).

TCA (Fig. 1) is composed of 4 sub-areas: Area I, Area II, Area III and Extended Petro Boundary. Methodology and findings from this study will be extrapolated or applied to other areas of Tambaredjo field and other fields (Tambaredjo North West and Calcutta), adapting these to the features of the mentioned areas or fields.

Heavy oil production from TCA comes from unconsolidated sands, the so-called T-sands, at average depth of 900 to 1,400 ft. The T-sands are of Paleocene age and of fluvial-estuarine to coastal marine of origin and consists of angular, medium to course drained unconsolidated sands with intercalated clays and lignites. The reservoir is sealed by locally continuous clays that overlap the Cretaceous surface in the South [6].

The sands are deposited on a well cemented erosional Cretaceous basement, during an overall transgressive period, as multilateral and vertically stacked sand bodies. Fig. 2 illustrates the geological conceptual model of the T sand reservoirs of the T unit in the TAM field [6].

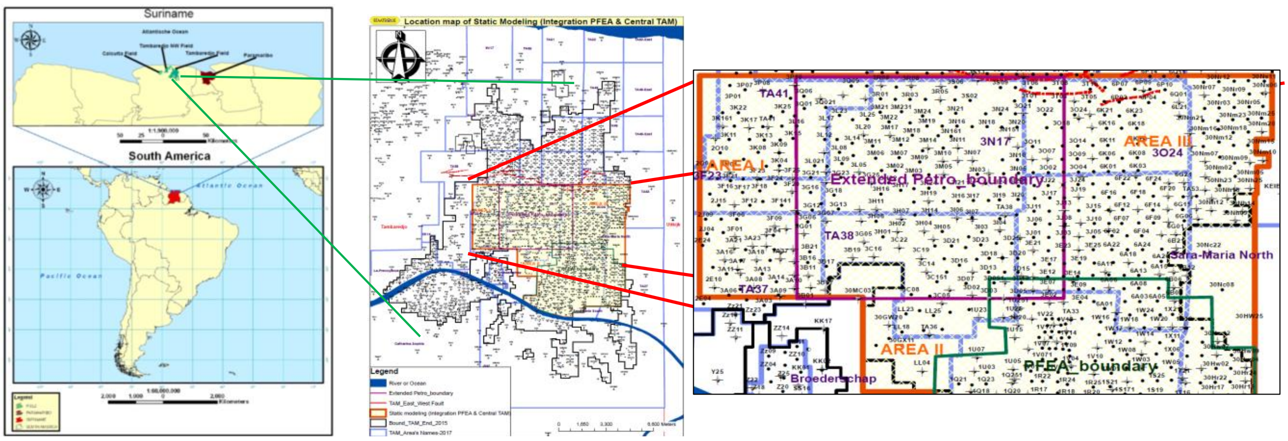

Fig. 1. Location map of Staatsolie oilfields (left) and of the TCA (Area I, II, III and Extended Petro Boundary) [6].

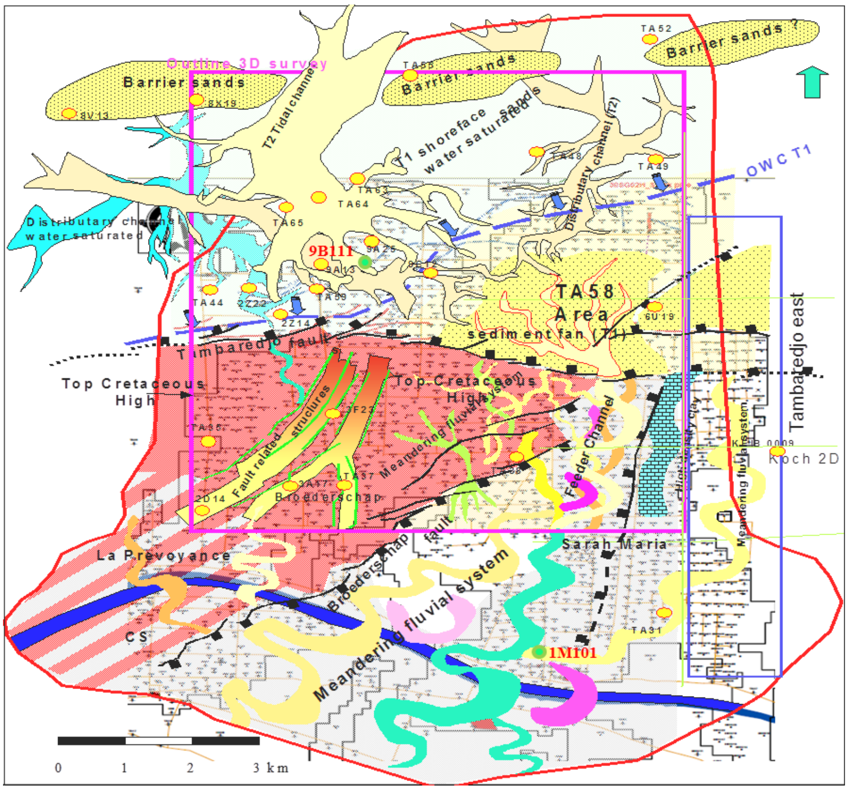

Fig. 2. Geological concept of the depositional environment of the Tambaredjo field [11].

3 Previous studies

Appendix A summarizes previous studies done regarding the determination of tortuosity (a) and cementation factor (m). This summary was one of the key facts that led the authors to search for a practical method to estimate a and m as variables related to heterogeneity.

As presented in this table (Appendix A), a and m vary with lithology and geological facies.

Pinas and Acosta [10] demonstrated the impact of varying a and m on S_w in the Tambaredjo field. The differences found was ±11.89% when using maximum and minimum core values for a and m.

4 Methodology

Fig. 3 summarizes the activities done for determining tortuosity (a) and cementation factor (m) as variables for TAM Central Area (TCA).

Items 2 and 3 of the workflow are explained in this section and preliminary results are presented. Items 4 and 5 are explained in the Results Analysis section.

4.1 Data gathering, validation and preliminary calculations

4.1.1 Core data

Clay volume (V_{cl}) from X-Ray Diffraction (XRD) data from 2 wells (9B111 and 1M101) was used to calibrate log derived V_{cl}.

Special Core Analysis (SCAL) data from 2 wells (9B111 and 1M101) consisting of: formation factor (F_a), cementation exponent (m), air permeability (K_a) and porosity. This data was used to calibrate the indexes, comparing core derived indices to log derived indices.

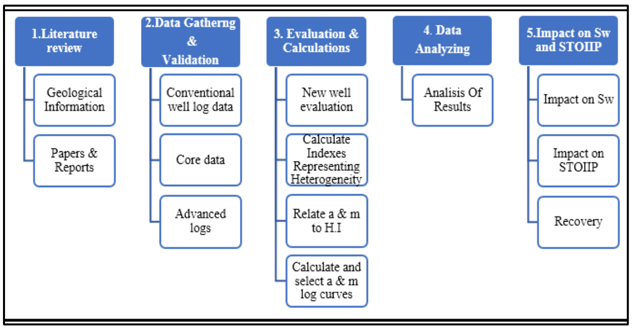

Fig. 3. Workflow for determining S_w Equation.

Permeability corrected (Klinkenberg) and porosity from conventional plug analysis data of 7 wells (I211, 9B08, 6P22, 3D19RE, 3Z24, 9B111, 1M101), were used as input to calculate the indexes representing heterogeneity.

LPSA (Laser Particle Size Analysis) data of 7 wells (I211, 9B08, 6P22, 3D19RE, 3Z24, 9B111, 1M101) consisting of: clay volume, silt volume, permeability, porosity and Folk, Moment and Trask indexes for sorting. The data was reported and named according to the depth at which each sample was taken.

4.1.2 Conventional logs

Well log data (532 wells) consisting of gamma ray logs, neutron logs, density logs and resistivity logs.

- Log data of 500 wells that were evaluated within the TCA were used for water saturation (S_w) estimation.
- 30 additional wells located North of TCA were evaluated during this study. The log data was used to calibrate the S_w, as these wells have an Oil Water Contact (OWC), meaning that S_w should be close to 100% in these water zones.
- Log data of the 2 cored wells (9B111 and 1M101) within TCA were used to calibrate the *a* and *m* curves. Both wells were already evaluated, and the well log data was directly used.

4.2 Heterogeneity Indexes calculation

An approach towards determining *a* and *m* as variables is by finding an index that represents the formation's heterogeneity. The following table (Table 1) summarizes the indexes used: heterogeneity index (HI, input parameters and Pore Throat Size (PTS).

Table 1. Heterogeneity indexes (HI).

Index	Equation	Reference	Features
BPPI (Basic Petrophysical Property Index)	$BPPI = \frac{\emptyset_e}{1-\emptyset_t} \times (1 - V_{sh})$	Angel [12]	Ratio of volume of fluids in the interconnected pore space to the volume of solid rock
NRI (Net Reservoir Index)	$\mathrm{NRI} = \frac{\emptyset_t \times V_{sh}}{1-\emptyset_t} \times \emptyset_e$		Relationship between BPPI and PHIE.
Rock Texture	$\text{Rock Texture} = \frac{\phi^3}{1-\phi^2}$	Kozeny [13] and Carman [14]	Term from the Kozeny-Carmen Equation used for pressure drop in porous medium
RQI (Roc Quality Index)	$\mathrm{RQI} = 0.0314\frac{K^{0.5}}{\phi}$	Jude and Mehmet [15]	Hydraulic flow unit used for flow unit's identification
PHIZ (Pore Grain volume Ratio)	$\mathrm{Phiz} = \frac{\phi}{1-\phi}$	Amaefule and Altunbay [16]	The ratio of pore volume to grain volume
FZI (Flow Zone Indicator)	$\mathrm{FZI} = \frac{RQI}{Phiz}$		Fluid flow in a porous medium, based on modified Kozeny-Carmen Equation

Table 2 lists the used input parameters, which are basically modification features used in several S_w equations (e.g. Indonesian [7], Modified Indonesian [17], Simandoux [18], Modified Simandoux [19], Acosta and Rosales [20]) based on the clay and shale deposition.

Table 2. Reservoir Properties related to heterogeneity.

Input Parameters	
V_{cl}	V_{sh}
1-V_{cl}	1- V_{sh}
1- V_{cl} ^2	1- V_{sh} ^2
1- V_{cl} /2	1- V_{sh} /2
1+ V_{cl} /2	1+ V_{sh} /2

Calculations of the PTS were also included in this study, this was done using the R55 formula recommended for rock type classifications for TCA (Table 4).

Table 3. R55 formula used for PTS determination [21].

Index	Equation	Reference	Features
PTS	$\text{Log R55} = 0{,}948 + 0{,}632 \times \text{Log K} - 1{,}426 \text{ Log } \phi$	**Kolodzie [22]** and **Pittman [23]**	R55 is the corresponding pore throat radius (PTS) at 55% of mercury saturation. Recommended for TCA.

From Laser Particle Size Analysis (LPSA) data, distribution statistics is used to obtain indexes for grain sorting. Folk, Moment and Trask are the 3 statistical methods used for delivering sorting indexes [24].

LPSA indexes were plotted against those of Table 1, Table 2 and Table 3 to obtain a relationship between grain distribution and formation heterogeneity (index of the rock quality regarding heterogeneity). A total of 115 correlation cross plots were made [25]. Table 4 groups the indexes according to the terms they represent.

Table 4. Index grouping according to grain size and pore size [25].

Representing	
Grain Distribution (y-axis)	**Heterogeneity** (x-axis)
Sorting Indexes	HI Indices
	Input parameters
	PTS

Fig. 4 shows the calculated BPPI (red dots) using core data for well 9B111.

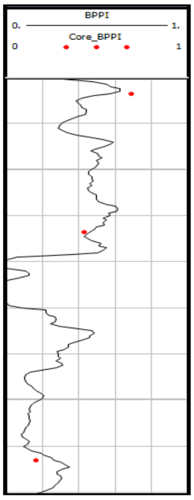

Fig. 4. Example of calibration of log calculated to core calculated BPPI on well 9B111

4.3 Tortuosity and cementation exponent relationships with Heterogeneity Index

m is determined for each plug sample analyzed assuming *a* =1 from equation (2).

$$F = \frac{a}{\phi^m} \quad (2)$$

Where: F = formation factor (dimensionless); ∅ = porosity (v/v); m = cementation factor (dimensionless); a = tortuosity factor (dimensionless)

In this research the semi-forced regression fitting was introduced to obtain different *a* values for each core sample with electrical properties. Application of this statistical processing technique for sample groups, resulted in *a* and *m* values for each group by adding 1 extra (1.1) coordinate to the dataset (Fig. 5).

Rearranging equation (2) delivers an equation for obtaining the tortuosity factor:

$$a = F \times \phi^m \quad (3)$$

Where: F = formation factor (dimensionless); ∅ = porosity (v/v); m = cementation factor (dimensionless); a = tortuosity factor from regression line (dimensionless)

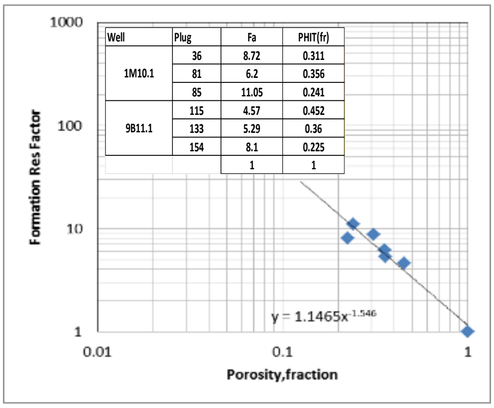

Fig. 5. Semi forced regression fitting cross plot (well 1M101 and 9B111).

Separate F-ϕ cross plots were made using data of well 1M101 and 9B111. Values for the *m* were obtained by applying both the free regression [5] and semi-forced regression approach, delivering 4 values for *m* (Fig. 6 and Fig. 7).

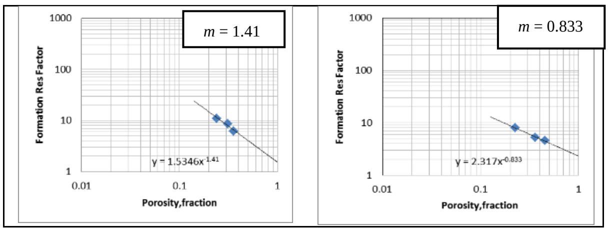

Fig. 6. Free regression fitting crossplot for well 1M101 (left graph) and 9B111 (right graph).

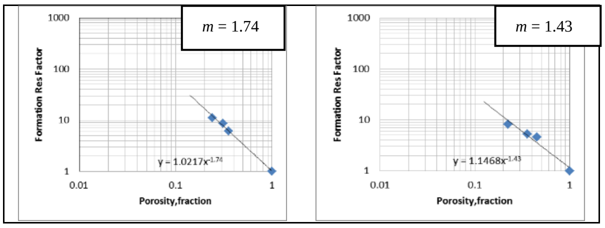

Fig. 7. Semi-forced regression fitting crossplot for well 1M101 (left graph) and 9B111 (right graph).

Using equation (3) and the four obtained values (Fig. 6 and Fig. 7), the *m* values for the tortuosity factor were back calculated. The usage of the cementation factor value depends on the well and the approach used for obtaining it. The free tortuosity factor refers to the *a* calculated using *m* from the free regression [5] approach and the semi-forced tortuosity factor refers to the a calculated using *m* from the semi-forced tortuosity factor (Table 5).

Table 5. Core *m*, free regression and semi-forced calculated *a*, reservoir properties and HI for core plug samples.

			Regression				
			Free	Semi-forced			
Well	Sample	m	a	a	V_{cl} (v/v)	V_{sh} (v/v)	BPPI
1M101	36	1.85	1.68	1.143	0.124	0.277	0.29
	81	1.77	1.45	1.028	0.094	0.276	0.36
	85	1.69	1.49	0.929	0.104	0.294	0.2
9B111	115	1.91	2.36	1.468	0.034	0.129	0.69
	133	1.63	2.26	1.227	0.041	0.199	0.43
	154	1.4	2.34	0.96	0.131	0.373	0.16

From left to right: Column 1: Well name; Column 2: Plug sample number; Column 3: Cementation factor from core; Column 4: tortuosity factor using free regression approach; Column 5: Tortuosity factor using semi-forced regression approach. Column 6: Clay volume from core data or calibrated log data; Column 7: Shale volume from core or calibrated log data; Column 8: Basic petrophysical property index calculated using core data or calibrated log data

Correlation cross plots were made by plotting data of Table 5 (*a* and *m* vs. V_{cl}, V_{sh} and BPPI) [25] where each *m* and *a*, were plotted as a function of V_{cl}, V_{sh} and BPPI (which were considered the preliminary selections based on the criteria of $R^2 > 0.75$ and logical trend (matching lithology).

4.4 Selection of tortuosity and cementation factor log curves

The analysis of the preliminary results plotted as log curves [25] led to some questions. The determination of *a* and *m* maybe should be estimated by pair as they should be inverse proportional according to the free and semi-forced regression crossplots. None of the sets of curves created could totally fulfill the criteria even though some were showing very good match with core data. Considering this and that because of the unconsolidated nature of the reservoir, samples in good rock quality intervals could not be retrieved, a different approach was needed.

Using the R55 formula (Table 3) for PTS calculation and the classification ranges (Table 6), the core samples were classified by rock type numbers (Table 7). Rock type 0 is the best possible rock quality and rock type 5 is the worst.

Table 6. Rock type classification ranges [26].

Rock Type	PTR [microns]
RT0	PTR > 30
RT1	20 < PTR < 30
RT2	14 < PTR < 20
RT3	8 < PTR < 14
RT4	3 < PTR < 8
RT5	PTR < 3

Rock type classification according to the pore throat radius

Table 7. Core samples and their rock type number

Well	Plug	Rock Type
1M10.1	36	RT4
	81	RT3
	85	RT4
9B11.1	115	RT4
	133	RT5
	154	RT5

Core samples classified by rock type

Table 7 reveals, that the data set available is limited to rock type 3, 4 and 5, which is mainly silty-shaly sand. This data set does not accommodate for good quality reservoir sand (RT0). It was also noted that the data set neither covered shale nor clay. In other words, the full spectrum of rock types was not possible to use to estimate a and m for all the types present in the reservoir.

Compiling the data set to accommodate rock quality ranges from RT0 to shale:

1. For RT0, *a* and *m* values from literature, proposed for unconsolidated sands (Humble formula) were used (Table 8). The BPPI was estimated using average inputs for clean sands (V_{sh}< 5%).
2. For RT4 and RT5, the *a* and *m* values were obtained by F-ϕ cross plots (Fig. 8). The V_{sh} and V_{cl} values are averages from available core data and were used for BPPI calculations including ∅.
3. For shale, the *a* and *m* values were extrapolated using the trend equations for the parameters representing V_{sh}, V_{cl} and BPPI. BPPI was estimated using known values for shale.

Table 8. Data set for final *a* and *m* equations

	Free regression Fitting				
	Vsh	Vcl	BPPI	*m* (plot)	*a* (plot)
RT0 (Literature)	0.025	0.013	0.784	2.15	0.62
RT4	0.203	0.066	0.470	1.68	1.17
RT5	0.334	0.092	0.263	1.23	1.56
shale			0.02	0.99	2.35
		0.85		0.81	3.24
	0.95			1.11	1.93

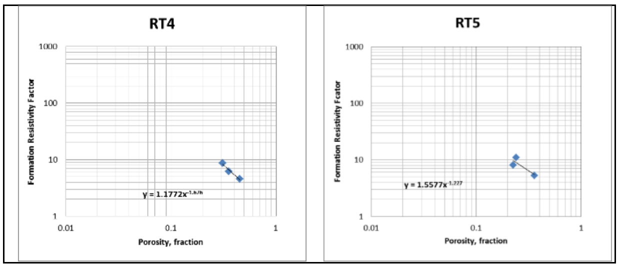

Fig. 8. F-ϕ cross plots for RT4 and RT 5.

Porosity versus Formation resistivity factor cross plots using data of the samples classified as RT 4 and RT5

Plotting the data of Table 8 (Figs. 9, 10 and 11), equations for *a* and *m* were obtained. Each parameter was plotted as a function of V_{sh}, V_{cl} and BPPI.

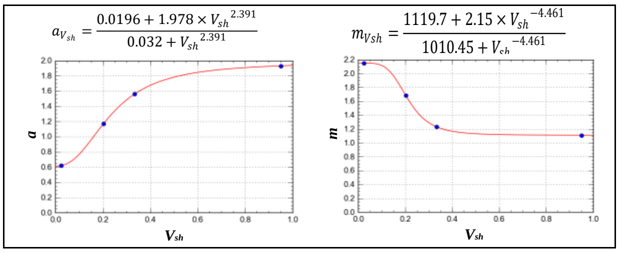

Fig. 9 Crossplots of *a* and *m* as functions of V_{sh}.

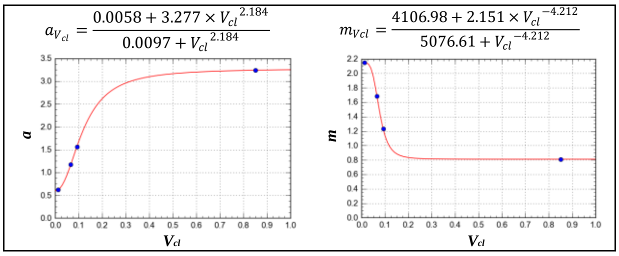

Fig. 10. Crossplots for *a* and *m* as functions of V_{cl}.

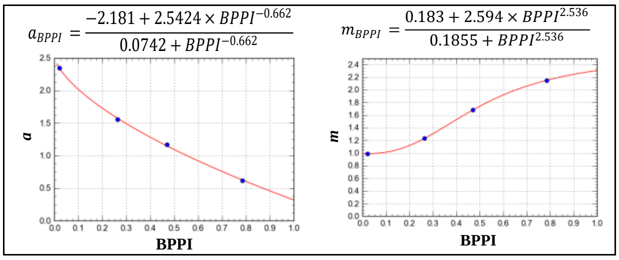

Fig. 11 Crossplots for a and m as functions of BPPI.

The log curves for *a* and *m* were created for each well (e.g. 1M101 Fig. 12: tracks on the right). The *a* from core is indicated by the red dots and the *m* from core is indicated with the black dots.

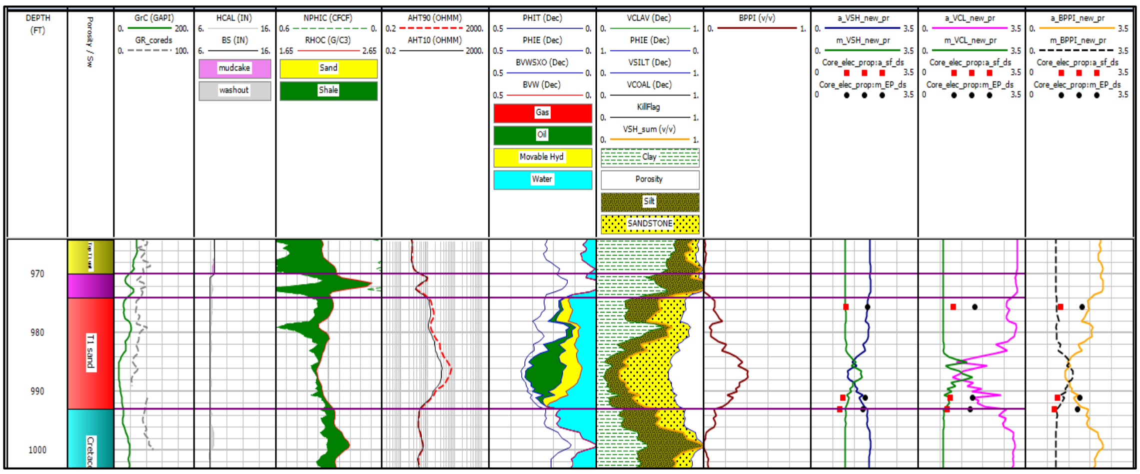

Fig. 12. Petrophysical evaluation with imported *a* and *m* curves (before adjustments) for well 1M101.
From left to right: Track 1: Depth reference; Track 2: Formation tops zonation; Track 3: Gamma ray; Track 4: Caliper and Bit size; Track 5: Neutron & Density; Track 6: Resistivity curves; Track 7: Porosity calculations; Track 8: Lithology composite; Track 9: Basic Petrophysical Property Index; Track 10: a & m as a function of V_{sh} (red squares: core tortuosity and black circle: core cementation factor); Track 11: a & m as a function of V_{cl} (red squares: core tortuosity and black circle: core cementation factor); Track 12: a & m as a function of BPPI (red squares: core tortuosity and black circle: core cementation factor)

5. Results analysis

In this section the results of the approach to determine *a* and *m* as variable parameters are presented and discussed, establishing S_w calculations using *a* and *m* log curves that depend on reservoir heterogeneity.

5.1 Indexes representing formation heterogeneity

Out of the 115 correlation cross plots made [25], three indexes were selected based on the criteria of R^2>0.75 and logical trend line. These are:

- V_{cl} with R^2 = 0.829 (Fig. 9)
- V_{sh} with R^2 = 0.849 (Fig. 10)
- BPPI with R^2 = 0.936 (Fig. 11)

Even though V_{sh} and V_{cl} are not really indexes, they do express in a certain form the reservoirs heterogeneity. These and BPPI show good correlations between grain distribution and heterogeneity.

5.1.1 Final selection and adjustments for the curves

Adjustments were made to the correlations (Figs. 9, 10 and 11) to match core data. Adjustments required for well 1M101 (Fig. 13) to match the core data, were not the same adjustments required for well 9B111 (Fig. 14).

An analysis was done exploring to explain these two sets of adjustments. The locations of both wells (9B111 and 1M101) were reflected to a geological concept of the depositional environment of the Tambaredjo field, showing clearly that both wells are in 2 different depositional environments (Fig. 2). Well, 1M101 was drilled in a meandering fluvial system, while 9B111 is in a deltaic system. Depositional facies for each system are very different and this explains the necessity of different adjustments to match core data for each well. Before taking the final decision of which correlation set of curves to select, it was obvious that these would need to be applied by areas according to the well location. In other words, wells in Tambaredjo Central should use correlation set for a and m curves with adjustments made for well 1M101 and wells in Tambaredjo North should use correlation set for *a* and *m* curves with adjustments made for well 9B111.

The correlation set curves were selected using the following criteria:

- *a* and *m* curves must be variable within the depth, avoiding straight vertical lines in the reservoir.
- Values of *a* must be inversely proportional to the values of *m*, when one increases in value, the other should decrease in value (according to the free regression crossplot approach).

The ultimate selection of *a* and *m* curves are the ones representing BPPI (Equations (6) and (7) for well 1M101; and Equations (8) and (9) for well 9B111) (further referred to as variable *a* and *m*), highlighted with red rectangle box in Fig. 13 and Fig. 14 (Track 11). S_w was then calculated using the field average of *a* = 1 and *m* = 1.66 (further referred to as average *a* and *m*) and compared to S_w calculated using variable *a* and *m*. The green triangle represents S_{wir} from core data.

$$a_{BPPI} = \frac{-2.181+2.242\times BPPI^{-0.662}}{0.0742+BPPI^{-0.662}} - 0.55 \qquad (6)$$

$$m_{BPPI} = \frac{0.183+2.594\times BPPI^{1.836}}{0.1855+BPPI^{1.836}} + 0.4 \qquad (7)$$

$$a_{BPPI} = \frac{-2.181+2.242\times BPPI^{-0.662}}{0.0742+BPPI^{-0.662}} - 0.05 \qquad (8)$$

$$m_{BPPI} = \frac{0.183+2.594\times BPPI^{1.836}}{0.1855+BPPI^{1.836}} - 0.15 \qquad (9)$$

Where: a_{BPPI} = Tortuosity as function of BPPI (dimensionless); m_{BPPI} = Cementation Factor as function of BPPI (dimensionless); BPPI = Basic Petrophysics Properties Index

For both wells (Track 15 in Fig. 13 and Fig. 14) the continuous curve is the calculated S_w using average *a* and *m* and the dotted curve is S_w calculated using variable *a* and *m*, showing a slight decrease in S_w in the reservoir zones (T1 and T2 sands).

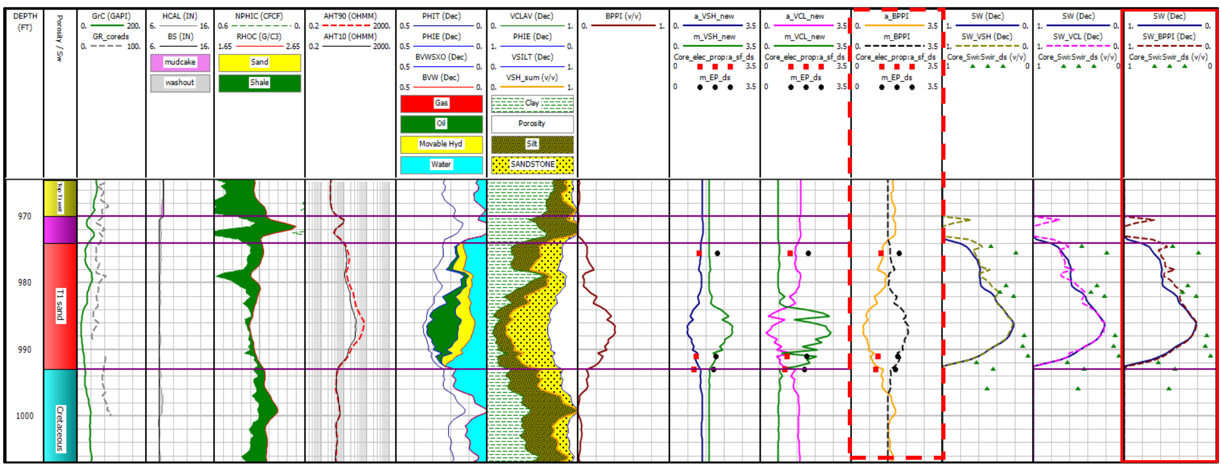

Fig. 13. Petrophysical evaluation with ultimate *a* & *m* curves adjustments for well 1M101.

* Corresponding author: eacosta@staatsolie.com

From left to right: Tracks 1 to 12 as per Figure 12: Track 13: S_w using fixed a & m values compared to S_w using a & m from V_{sh} and S_{wir} from relative permeability analysis (green triangles); Track 14: S_w using fixed a & m values compared to S_w using a & m from V_{cl} and S_{wir} from relative permeability analysis (green triangles); Track 15: S_w using fixed a & m values compared to S_w using a & m from BPPI and S_{wir} from relative permeability analysis (green triangles).

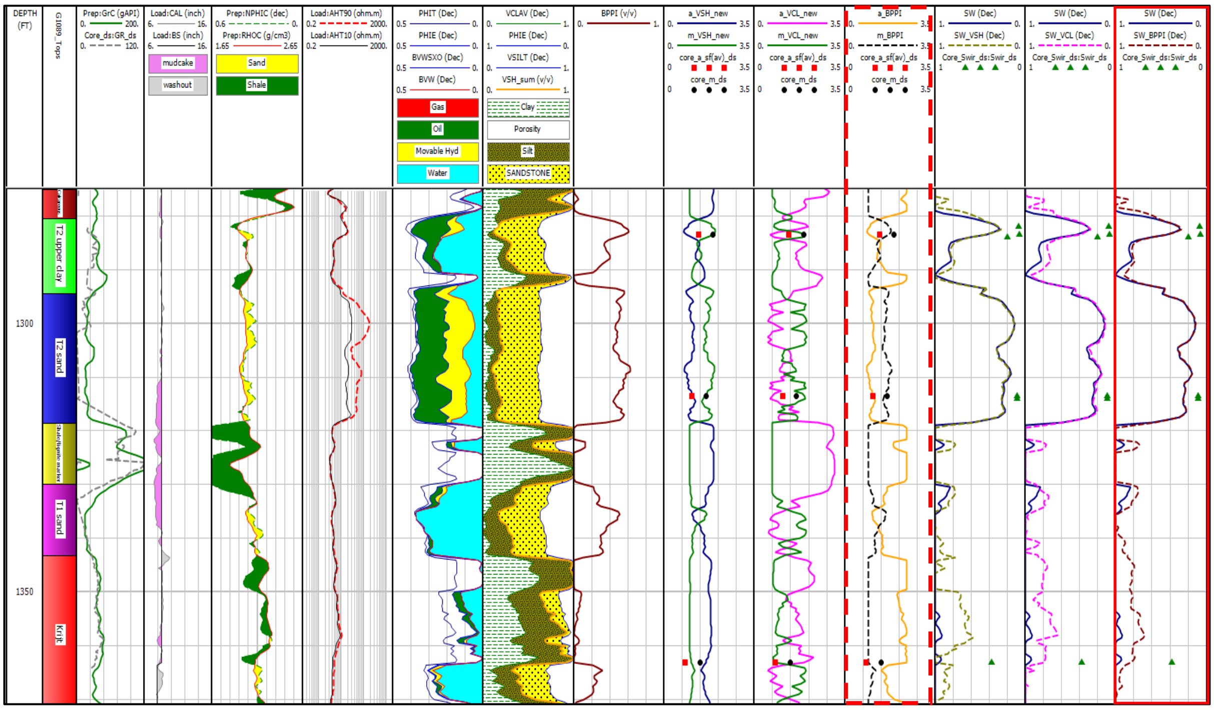

Fig. 14. Petrophysical evaluation with ultimate *a* & *m* curves adjustments for well 9B111.
From left to right: Tracks 1 to 12 as per Figure 12: Track 13: S_w using fixed a & m values compared to S_w using a & m from V_{sh} and S_{wir} from relative permeability analysis (green triangles); Track 14: S_w using fixed a & m values compared to S_w using a & m from V_{cl} and S_{wir} from relative permeability analysis (green triangles); Track 15: S_w using fixed a & m values compared to S_w using a & m from BPPI and S_{wir} from relative permeability analysis (green triangles)

Some wells were selected randomly for discussion. S_w was calculated, using both average and variable *a* and *m* values.

Well 3E141 (Fig. 15) is located South West in Area III and was evaluated using well 1M101 variable *a* and *m* adjustments. Displayed in track 7 is the lithology volumetrics (sand, silt, clay and porosity) for the T-unit reservoirs. In this well, the T1 sand is the cleanest sand according to the maximum clay volume of 0.2%. The S_w curves in track 10 show a reduction of 6.8% in the T1 sand, 4.4% in T2 sand and 0.4% in T3 sand. As observed, the calculated S_w using average *a* and *m* values, is mostly overestimated in the T1 sand which is the cleanest sand.

Well 3Z24 (Fig. 16) is located North outside of Area III and was evaluated using well 9B111 variable a and m adjustments. Displayed in track 7 is the lithology volumetrics (sand, silt, clay and porosity) for the T-unit reservoirs. The S_w curves in track 10 show an average reduction of 3.1% in the T1 sand, 4.1% in T2 sand and 5.3% in T3 sand.

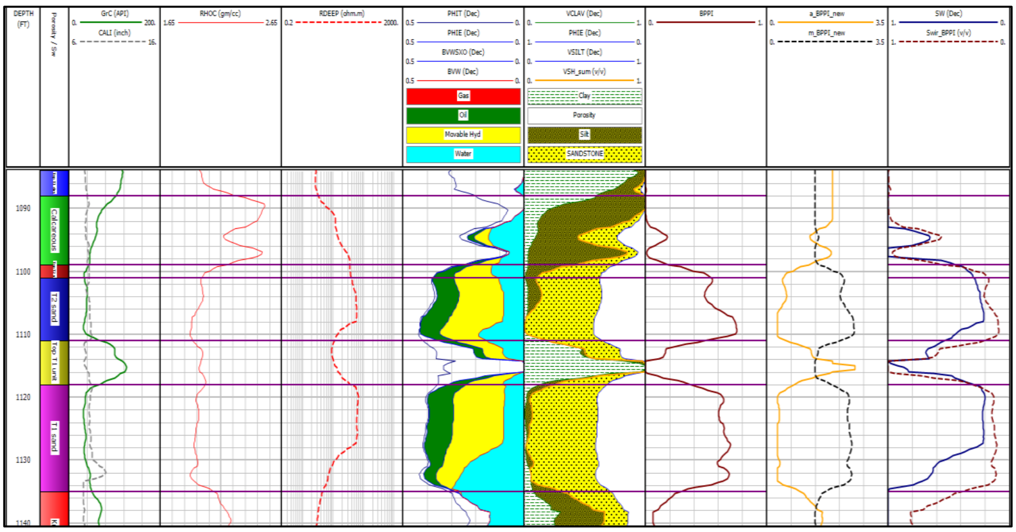

Fig. 15. Petrophysical evaluation of well 3E14.1 located in Area III and using well 1M101 parameter adjustments.
From left to right: Track 1: Depth reference; Track 2: Formation tops zonation; Track 3: Gamma Ray & Caliper; Track 4: Neutron & Density; Track 5: Resistivity curves; Track 6: Porosity calculations; Track 7: Lithology composite; Track 8: Basic Petrophysical Property Index; Track 9: a & m as a function of BPPI; Track 10: S_w using fixed a & m values compared to S_w using a & m from BPPI.

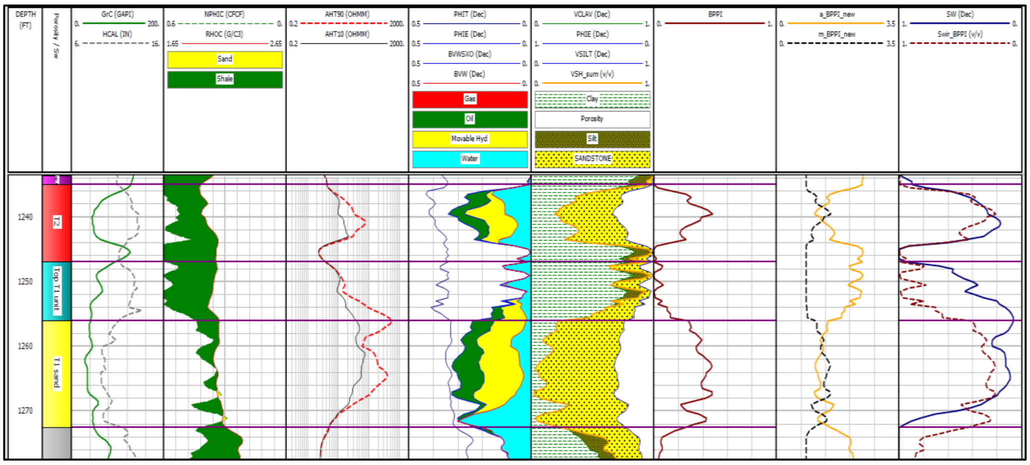

Fig. 16. Petrophysical evaluation of well 3Z24.1 located in Area III and using well 9B111 parameter adjustments.
From left to right: Track 1: Depth reference; Track 2: Formation tops zonation; Track 3: Gamma ray; Track 4: Neutron & Density; Track 5: Resistivity curves; Track 6: Porosity calculations; Track 7: Lithology composite; Track 8: Basic Petrophysical Property Index; Track 9: a & m as a function of BPPI; Track 10: S_w using fixed a & m values compared to S_w using a & m from BPPI.

5.2 Impact on water saturation

Water saturation for the T-unit was calculated and analyzed using histograms (Figs. 17, 18 and 19). Discriminators ($V_{cl} \leq 50\%$ and $R_t \geq 10$ ohm.m) were applied to analyze the impact of the variable *a* & *m* in S_w only in the reservoir intervals. Following histograms for Area III are discussed. All other areas histograms can be found in the Appendix (B, C and D).

The T1 histograms (Fig. 17) comparison for calculated S_w show a mean decrease of 6.96% when S_w is calculated using variable *a* and *m*, instead of the average *a* and *m* values.

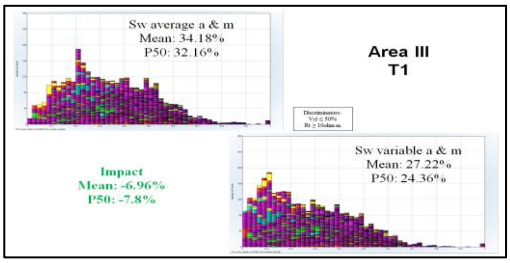

Fig. 17. S_w histogram comparison of theT1 sand (Area III

The T2 sand histograms (Fig. 18) comparison for calculated S_w show a mean decrease of 5.66%, when S_w is calculated using variable *a* and *m*, instead of the average values.

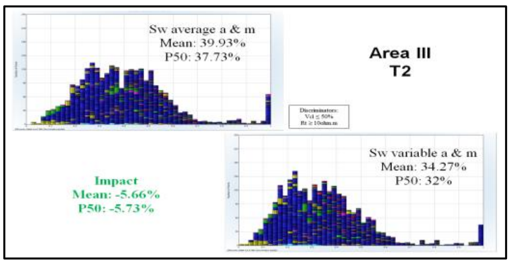

Fig. 18. S_w histogram comparison of the T2 sand Area III.

The T3 sand histograms (Fig. 18) comparison for calculated S_w show a mean decrease of 9.61% when S_w is calculated using variable *a* and *m*, instead of the average values.

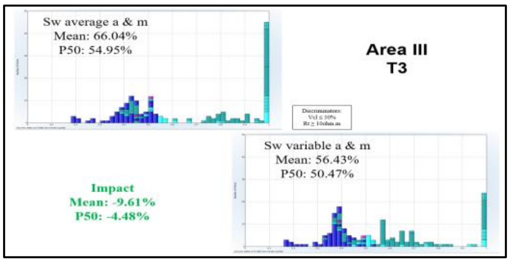

Fig. 19. S_w histogram comparison of theT3 sand (Area III).

S_w estimations for Area III using average *a* and *m* values, was mostly overestimated in the T1 sand which is the cleanest reservoir sand within Area III. The more the reservoir was rich in clay, the smaller was the difference in S_w calculations using average and variable *a* & *m* values. When comparing T1 versus T2 sands, they differ in reservoir quality. The mean V_{cl} for the T1 is 18% and the $\emptyset_e$ is 28% and the mean V_{cl} for the T2 is 28% and the $\emptyset_e$ is 25%. Calculated S_w using the variable *a* & *m* values is notably corrected in the clean reservoir sands (T1) compared to the more clay rich sands (T2 and T3). T3 histogram comparison shows the highest improvement, and this can be associated to the update of clay endpoints and re-zonation.

It is important to highlight the fact that good reservoir quality intervals (RT0, RT1, RT2) (Table 7) will have their S_w calculations improved as previous average values ($a = 1$ & $m = 1.66$) were related to rock types classified as RT3, RT4 and RT5, which are mainly shaley sandstones to shale rocks.

A summary of analyzed statistical data from the T1, T2 and T3 sands for all the 4 areas from TCA are presented in Table 9. Average decrease in S_w is from 42% to 37% with improvements varying from 6 to 20%.

Table 9. Summary of S_w histogram comparison for all Areas (TCA) using fixed and variable *a* and *m*.

Sw Models	Area I Sw(%)			Area II Sw(%)			Area III Sw(%)			Extended Petro. Sw(%)		
	T1	T2	T3	T1	T2	T3	T1	T2	T3	T1	T2	T3
Indonesian/a:1 & m:1.66 /Rw:1.18 @ 67°F	33.9	34.8	43.0	43.9	31.6	53.9	34.2	39.9	66.0	39.3	36.0	46.3
Indonesian/a & m: variable /Rw: 1.18 @ 67°F	31.0	31.7	39.5	41.3	29.4	48.7	27.2	34.3	56.4	33.6	29.5	41.7
Difference (%):	-2.8	-3.2	-3.5	-2.6	-2.2	-5.2	-7.0	-5.7	-9.6	-5.7	-6.5	-4.6
Improvement (%):	**-8.3**	**-9.1**	**-8.1**	**-5.9**	**-7.0**	**-9.7**	**-20.4**	**-14.2**	**-14.6**	**-14.4**	**-18.0**	**-10.0**

5.3 Impact on Stock Tank Oil Initially In Place

Since the commercial purpose is to know the current reserves volume, before going to production, determining accurate water saturation for a reservoir is vital. S_w is used to calculate the oil saturation ($S_o = 1\text{-}S_w$), which is the real quantity of interest. STOIIP estimations were made for all studied areas (Area I, Area II, Area III & Extended Petro.) using the S_w calculated with fixed average a and m values and compared to estimations using S_w calculated with variable *a* and *m* (Table 10). Estimates were done only for T1 and T2 sands, as previous estimates for Static Model update, Material Balance and Simulation only involve these reservoirs.

Table 10. STOIIP estimations for the T-unit sands from all TCA areas using variable *a* & *m.*

Area	Reservoir	Updated Sw using variable a & m				
		Net Volume MM ft3	Pore volume MM RBls	Sw v/v	So (1-Sw) v/v	STOIIP MMBls
I	T2 Sand	572.81	32.93	0.317	0.683	**22.18**
	T1 Sand	173.82	9.71	0.31	0.69	**6.61**
II	T2 Sand	430.92	23.71	0.294	0.706	**16.51**
	T1 Sand	281.14	15.07	0.413	0.587	**8.72**
III	T2 Sand	1638.17	86.54	0.343	0.657	**56.07**
	T1 Sand	1215.35	67.45	0.272	0.728	**48.43**
Ext. Petro	T2 Sand	1988.86	109.75	0.295	0.705	**76.31**
	T1 Sand	1073.78	60.91	0.336	0.664	**39.89**
		7375	406	0.323	0.678	**274.71**

From left to right: Column 1: Study area analyzed; Column 2: Reservoir analyzed; Column 3: Net volume (in millions of cubic feet); Column 4: Pore volume (in millions of reservoir barrels); Column 5: Average water saturation using average variable a & m values; Column 6: Average oil saturation using variable a & m; Column 7: Stock tank oil initially in place using variable a & m

Table 11 shows how STOIIP estimations are in comparison with the actual recovery of TAM Central. Ambastha [27] and Lyons, et al. [28] refer to the following ranges regarding primary oil production for heavy oil: 5 to 10% and 7 to 13% respectively. 13.7% found is comparable with Lyon's range but out of Ambastha's.

Table 11. STOIIP estimations comparison and actual recovery for T1 and T2 sands of TCA

Model	Average S_w (%)	STOIIP (MMbbls)	Actual recovery (%)*
Static update	66	175	21.5
Material Balance	----	195	19.3
Simulation	----	209	18.0
Static update including S_w	36.7	252	14.9
Variable *a* & *m*	32.3	275	13.7

*estimated with 37.62 MMbbls (October 2018)

Conclusions

- The Basic Petrophysics Property Index (BPPI) appears to be the most suitable Heterogeneity Index (HI) for estimating tortuosity (*a*) and cementation factor (*m*) as variable parameters based on core data and the inverse proportionality of these.
- It was found that depositional environment is an important feature to consider when relating *a* & *m* to heterogeneity as different set of adjustments were applied to the two core data set during calibration (well 1M101 in a fluvial system and 9B111 in a deltaic system).
- When formation heterogeneity is reflected in variable *a* and *m*, water saturation (S_w) improves in average from 41.9% to 38%. Considering only the T1 and T2 reservoirs intervals, STOIIP estimation in terms of actual recovery (using 37.62 MMbbls as of October 2018) represents 13.7%, which is now matching better the expected primary recovery.
- Despite of the low quantity of core data regarding electrical properties, properly relating these to reservoir heterogeneity allows improvements in S_w with higher impact in good quality reservoir rock (better properties), as now the variable *a* & *m* are not a value related to regular to poor quality rock (current core data average), only samples tested due to unconsolidation of the formation.

The authors would like to acknowledge F. Graanoogst (Petrophysics Specialist), P. Naigi (Sr. Petrophysicist), J. Oedietram (Sr. Petrophysicist), R. Ramdajal (G&G Teamleader), B. Nandlal (Functional Subsurface Support Division Manager) for their comments and encouragement during this project.

References

1 G. M. Hamada, A. Almajed, T. Okasha, and A. Algathe, Uncertainty analysis of Archie's parameters determination techniques in carbonate reservoirs: Journal of Petroleum Exploration and Production Technology, November, pp.1-10 (2012)

2 J. H. Schon, Physical properties of Rocks, Elsevier, pp. 273 – 336 (2011)

3 A. M. Attia, Effects of petrophysical rock properties on tortuosity factor. Journal of Petroleum Science Engineering, 48 (3-4), pp 185-198 (2005)

4 D. Tiab and E. C. Donaldson, Petrophysics: Theory and practice of measuring reservoir rock and fluid transport properties, 3rd ed. Gulf Professional Publishing. Houston, Texas, USA. pp. 976 (2012)

5 M. El Sharawy and B. S. Nabawy, Determining the porosity exponent m and lithology factor a for sandstones and their control by overburden pressure: AAPG Bulletin, pp. 1893-1910 (2018)

6 E. R. Acosta, A. Mijland and B. Nandlal, Detailed assessment for water saturation equations for determining the proper S_w model for unconsolidated sandstones in Tambaredjo field, Suriname. 22nd ICGPE. July 15-16, 2020 at Copenhagen, Denmark. pp. 371, 372. (2020).

7 A. Poupon and J. Leveaux, Evaluation of water saturation in shaly formations. *SPWLA 12th Annual Logging Symposium Transactions* (1971).
8 G. E. Archie, The electrical resistivity log as an aid in determining some reservoir characteristics: AIME Transactions, 146, pp. 54-62. (1942)
9 E. R. Acosta and E. Rosales Z., Tortuosity and Cementation Factor Parameters: A Review on their Determinations. Researchgate.com (2017)
10 M. Pinas and E. R. Acosta, Impact of tortuosity and cementation factor in water saturation calculations in heterogeneous sands of the Tambaredjo Field, Guiana Basin, Suriname. Researchgate.net (2019)
11 Staatsolie Maatschappij Suriname N.V., Development Drilling Program 2009 Tambaredjo Field. unpublished (2009)
12 F. Angel, Substituting Traditional Cutoff Parameters by a More Practical Novel Methodology for Estimating Net Pay Intervals in Shaly Sands, PDVSA (2018)
13 J. Kozeny, Ueber kapillare Leitung des Wassers im Boden. Sitzungsber Akad. Wiss., Wien, 136(2a): 271-306. (1927)
14 P. C. Carman, Flow of gases through porous media. Butterwoths, London, UK. (1956)
15 O. Jude and A. Mehmet, Enhanced Reservoir Description: Using core and log Data to Identify hydraulic (Flow) Units and Predict Permeability in Un-cored Intervals/Wells (1993)
16 O. Amaefule and M. Altunbay, SPE Enhanced Reservoir Description: Using Core and Log Data to Identify Hydraulic (Flow) Units and Predict Permeability in Uncored Intervals/Wells, SPE 26436 (1993)
17 R. Woodhouse, Athabasca Tar Sands Reservoir Properties Derived from Core and Logs. SPWLA 17th annual Logging Symposium Transactions (1976)
18 P. Simandoux, Dielectric measurements on porous media application to the measurement of water saturations: study of the behavior of argillaceous formations: Revue de l'Institut Francais du Petrole 18, Supplementary Issue, pp. 193-215 (1963)
19 C. Bardon and B. Pied, Formation water saturation in shaly sands: *SPWLA 10th Annual Logging Symposium Transactions*, Paper Z, 19 (1969).
20 E. R. Acosta, Petrophysical Model for High Irreducible Water Saturation Reservoirs in Oficina Formation (in Spanish). Master's Thesis. La Universidad del Zulia. Maracaibo, Venezuela (2006) http://dx.doi.org/10.13140/RG.2.2.22760.47369
21 Baker Hughes Inc., Field optimization using horizontal wells (feasibility study). Dynamic modelling. pp 47-56 unpublished (2015)
22 S. Kolodzie, Analysis of pore throat size and use of the Waxman-Smits Equation to determine OOIP in Spindle Field, Colorado. *SPE 55th Annual Fall Technical Conference*, Paper 9382, pp 10 (1980)
23 E. D. Pittman, Relationship of Porosity and Permeability to various Parameters Derived from Mercury Injection-Capillary Pressure Curve for Sandstone. AAPG Bulletin, **76** pp 191–8 (1992)
24 S. J. Blott and K. Pye, Gradistat: A grain size distribution and statistics package for the analysis of unconsolidated sediments. Surface Processes and Modern Environments Research Group, Department of Geology, Royal Holloway University of London, Egham, Surrey, TW20 0EX, UK, pp. 1237-1248. (2001)
25 M. Pinas, Determination of tortuosity (a) and cementation factor (m) as a variable parameter in T-Unit in Tambaredjo Central Field. BSc. Thesis. Anton de Kom Universiteit van Suriname. unpublished (2019)
26 J. Jowintinie, R. Ramadajal, A. Redjosentono, J. Oedietram, and E. Acosta, Advanced Facies Rock Typing Approach for 3D Geocellular Static Modeling for Polymer Flooding in the Tambaredjo Oil Field, Suriname. AAPG ICE 2019, Buenos Aires, Argentina, 27 – 30 August (2019)
27 A. Ambastha, SPE Reprint Series No. 61. Heavy oil recovery (2008)
28 W. Lyons, G. Plisga, and M. Lorenz, Standard Handbook of Petroleum and Natural Gas Engineering (Third Edition), pp. 225-228 (2016)
29 M. R. Wyllie and W. D. Rose, Some theoretical considerations related to the quantitative evaluation of the physical characteristics of reservoir rocks from electrical log data. AIME 189, pp. 105–118. (1950)
30 W. O. Winsauer, H. M. Shearin, P. H. Masson, and M. Williams, Resistivity of brine saturated sands in relation to pore geometry: American Association of Petroleum Geologists Bulletin, v. 36, no. 2, pp. 253-277 (1952)
31 J. E. Carothers, A statistical study of the formation relation: The Log Analyst, v. 9, p. 13−20. (1968)
32 C. R. Porter and J. E. Carothers, Formation factor-porosity relation from well log data: Soc. Professional Well log Analysts, 11th Annual Logging Symposium, Trans., Paper D (1970)
33 D. K Sethi, Some considerations about the formation resistivity factor-porosity relationships: Soc., Professional Well Log Analysts, 20th Annual Logging Symposium Trans., Paper L (1979)
34 G. V. Keller, Electrical properties of rocks and minerals. In: Carmichael, R.S. _Ed. Handbook of Physical Properties of Rocks, Vol. 1. CRC Press, Boca Raton, FL, pp. 217–293 (1982)
35 M. A. Lovell and P. A. Pezard, Electrical properties of basalts from DSDP Hole 504B: a key to the evaluation of pore space morphology, Geological Applications of Wire line Logs, Geological Society, London, pp. 339 – 345. (1990)
36 R. Ehrlich, E. L. Etris, D. Brumfield, L. P. Yuan, and S. J. Crabtree, Petrography and reservoir physics III — Physical models for permeability and formation factor. American. Association Petroleum Geologists. 75, pp. 1579–1592. (1991)
37 H. S. Salem and G. V. Chilingarian, The cementation factor of Archie's equation for shaly sandstone reservoirs: Journal of Petroleum Science and Engineering, March, pp. 83–93 (1999)
38 Schlumberger, A review of New Petrophysical Data and Analysis in the Tambaredjo field. (2009) unpublished
39 E. Larreal (2015), Petrophysical evaluation Suriname – Guyana Basin April, pp. 39 unpublished (2015)

Appendix

Appendix A. Summary of previous studies regarding *a* and *m* determination.

Researcher(s)	Year	Findings	Proposed		Comments
			a	***m***	
Archie [8]	1942	Values related to consolidation of the sandstone sample	**1**	**2**	For clean sands or carbonates
Wyllie and Rose [29]	1950	*m* shows wide variations from sample to sample, formation to formation, interval to interval in the same medium, and from medium to medium			
Winsauer, *et al.* [30]	1952	Generalized *a* from 1 to the term tortuosity factor, so that it could accommodate a variety of sandstone types	**0.62**	**2.15**	Also known as Humble. Unconsolidated sandstones
Carothers [31]	1968	Found different values for sands depending on the shalyness and lithologies	**1.45**	**1.54**	Average sands (fairly shaly)
			1.65	**1.33**	Shaly Sands
			1.45	**1.70**	Calcareous sands
			0.85	**2.14**	Carbonates
Porter and Carothers [32]	1970	Found new values for other formations	**2.45**	**1.08**	Pliocene sands, southern California. USA
			1.97	**1.29**	Miocene sands, Texas-Louisiana Gulf Coast. USA
Sethi [33]	1979		**1**	$\boldsymbol{\phi^{(2.05-\phi)}}$	
Keller [34]	1982	*m* is affected by lithology, porosity, pore throat size, degrees of compaction and cementation, and age			
Lovell and Pezard [35]	1990		**6.2**	**1.05**	
Ehrlich, *et al.* [36]	1991	*m* varies widely and changes continuously due to variations in depositional subfacies			
Salem and Chilingarian [37]	1999	*m* indicates reduction in pore openings. *a* has effect on various parameters such as porosity (ϕ), permeability (k), specific surface tension (s) and formation factor (F), hence, its effect on m is significant			
Acosta [20]	2006	S_w values could be overestimated from 6 to 18% when *a* and *m* values are different from recommended shaly sand ones	**1 to 1.65 depending on V_{sh} ranges**	**2 to 1.33 depending on V_{sh} ranges**	Oficina Formation, Eastern Basin Venezuela
Schlumberger [38]	2009	S_{wir} values are due to the wide variation in *m* and pore connectivity. An alternate way to estimate m was proposed using microresistivity	**1**	**1.69**	Tambaredjo field, Suriname
Schon [2]	2011	*a* and *m*, can be related to the pore geometry (texture) of the rock			
Hamada, *et al.* [1]	2012	*a* and *m* become more sensitive to pore pattern distribution and lithofacies properties			
Larreal [39]	2015	*m* varies from 1.48 to 1.72 within the region		**1.6**	Guyana Basin core data
Acosta and Rosales [9]	2017	S_w values could be overestimated from 6 to 18% when *a* and *m* values are different from recommended shaly sand ones	$\mathbf{0.285 \times Ln(V_{sh}) + 2.069}$	$\mathbf{-0.29 \times Ln(V_{sh}) + 0.899}$	Oficina Formation, Eastern Basin Venezuela
Pinas and Acosta [10]	2019	Values depend on the approach (free regression fitting or forced regression fitting) Different par of values for each cored well indicates field heterogeneity influence. Using fixed average values for the entire field will mislead S_w calculations.			Tambaredjo field, Suriname

Appendix B. Indonesian S_w histograms comparison using average vs. variable *a* and *m*. T-Unit sands. Area I

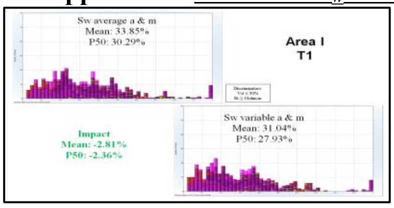

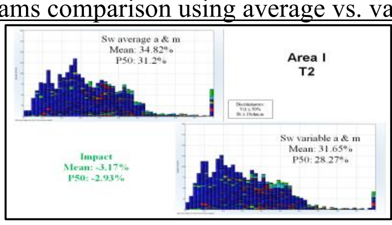

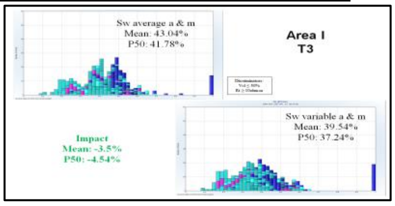

Appendix C Indonesian S_w histograms comparison using average vs. variable *a* and *m*. T-Unit sands. Area II

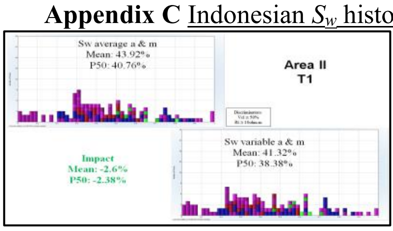

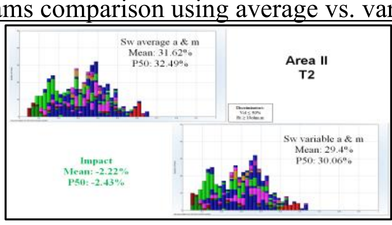

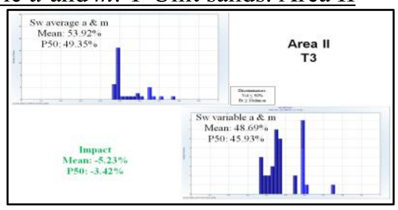

Appendix D Indonesian S_w histograms comparison using average vs. variable *a* and *m*. T-Unit sands. Extended Petro Boundary Area